Turk J Elec Eng & Comp Sci, Vol.20, No.Sup.1, 2012, © TÜBİTAK
doi:10.3906/elk-1101-1

# A novel approach for optimal allocation of distributed generations based on static voltage stability margin

**Mohsen Rezaie ESTABRAGH**[1], **Mohsen MOHAMMADIAN**[1,*], **Mehdi SHAFIEE**[2]
[1]*Department of Electrical Engineering, Sahid Bahonar University of Kerman, Kerman-IRAN*
*e-mails: m.mohammadian@uk.ac.ir, mohsenrezaie2009@gmail.com*
[2]*Department of Electrical Engineering, Amir Kabir University of Technology, Tehran-IRAN*
*e-mail: shafie@aut.ac.ir*

Received: 01.01.2011

**Abstract**

*This paper presents a newly developed approach to find the optimal location of distributed generations (DGs) to improve power system voltage stability margin and reduce losses incorporating the constraints. The loadability limit index is used to assess the static voltage stability security margin, which is associated with the point of voltage collapse limit. Based on this, a toolbox is developed to recognize the loadability margin in power networks. Finally, the mentioned problem is modeled as a nonlinear and multiobjective optimization problem. The proposed method establishes a tradeoff between the security index and power losses in DG placement using the hybrid particle swarm optimization (HPSO) algorithm method to reach the best performance and acceptable operation. The simulations are performed on IEEE 14- and IEEE 30-bus test systems to find the optimal location of the DGs. The results are compared with the particle swarm optimization (PSO) algorithm to ascertain the effectiveness.*

**Key Words:** *Distributed generations, static voltage stability, load ability limit, power loss, hybrid particle swarm optimization, nonlinear optimization*

## 1. Introduction

Several major blackouts have occurred due to voltage instability in recent years, causing the voltage instability phenomenon to draw more and more attention worldwide. Voltage stability is the ability of a system to maintain voltage and is closely associated with power delivering capability. The voltage instability phenomenon, which can occur in both transmission systems and distribution systems, may not be new to power system practicing engineers and researchers [1,2]. With development of the national economy and the improvement of people's lives, load demands on networks are sharply increasing and the operation conditions of transmission networks are much closer to the voltage stability boundaries. The decline of the voltage stability level is one of the important factors that restrict the increase of the load served by transmission companies. Therefore, it is necessary to consider voltage stability constraints for the planning and operation of transmission systems.

*Corresponding author: Department of Electrical Engineering, Sahid Bahonar University of Kerman, Kerman-IRAN

Regarding these matters, distributed generation (DG) is increasingly gaining great attention from engineers. The development of DGs will bring new opportunities for traditional distribution and transmission systems. There are many technical benefits of employing DGs in existing networks, such as reducing line losses, reducing the emission of pollutants, improving power quality, and relieving transmission and distribution congestion [3]. DG refers to small sources ranging between 1 kW and 50 MW electrical power generations, which are normally placed close to consumption centers. Specifically, DGs connected to networks have the potential to improve system voltage stability. The research on voltage stability can be classified into static and dynamic analysis [4-6]. DG renders a group of advantages, such as economic, environmental, and technical. The economic advantages are the reduction of transmission and distribution costs, reduction of electricity price, and saving of fuel. Environmental advantages entail reductions of sound pollution and emissions of greenhouse gases. The technical advantages cover a wide variety of benefits, such as line loss reduction, peak shaving, increased system voltage profile, and, hence, increased power quality and relieved transmission and distribution congestion as well as grid reinforcement. It can also provide stand-alone remote applications with the required power. Therefore, the optimal placement of DGs and optimal sizing attract active research interest. Several researchers have worked in this area [7-13].

DGs are placed at optimal locations to reduce losses [7]. Some researchers have presented power flow algorithms to find the optimal size of DGs at each load bus [8,9]. Wang and Nehrir have shown analytical approaches for optimal placement of DGs in terms of loss [10]. Chiradeja quantified the benefit of reduced line loss in a radial distribution feeder with a concentrated load [11]. Further, many researchers have used evolutionary computational methods for finding the optimal DG placement [14-19]. Mithulananthan used a genetic algorithm (GA) for placement of DGs to reduce the losses [15]. Celli and Ghiani used a multiobjective evolutionary algorithm for the sizing and placement of DGs [18]. Nara et al. used a tabu search algorithm to find the optimal placement of DGs [19]. The former is intended to evaluate the voltage stability margin based on power flow calculations. The latter is to clarify the process of the voltage instability phenomenon while the effect of various control equipment is taken into account.

Due to the discrete nature of the allocation and sizing problem, the objective function has a number of local minima. Since the analytical methods are generally poorly suited to this type of function, only a few papers have used these methods. Almost all of the related papers are based on heuristic methods. Among the proposed methods, the hybrid particle swarm optimization (HPSO) algorithm has emerged as a useful tool for engineering optimization, which has been used in complex optimization problems [20-25].

This paper presents a novel search approach with respect to the voltage stability margin for the optimal placement of DGs using the HPSO algorithm and compares it with the particle swarm optimization (PSO) algorithm. Optimal bus locations are determined to obtain the best objective. The multiobjective optimization simultaneously covers the optimization of both the voltage stability margin and active power loss. This paper uses static analysis to discuss the impacts of DGs on voltage stability in transmission systems. This static voltage stability analysis is based on nonlinear optimization. The analysis process is performed using a steady-state voltage stability index, $P_T$, which is maximum loading under the feasibility of power flow equations [26-30]. The problem is defined and the objective function is introduced to maximize the voltage stability index, $P_T$, and minimize losses. Hence, a toolbox is developed to assess the power system voltage stability margin based on the loadability limit. This method is executed on the IEEE 14- and IEEE 30-bus test systems, showing the robustness of this method in finding the optimal and fast placement of DGs, efficiency for improvement of voltage stability index $P_T$, and reduction of power losses.

# 2. Problem formulation

A multiobjective function is implemented in this section. The objects considered in this study, for finding the optimal placement of DGs, are maximizing the loadability limit and minimizing the total system power losses.

## 2.1. Maximize voltage stability index

### 2.1.1. Voltage stability index formulation

The decline of the voltage stability level is one of the important factors that restrict the increase of load served by distribution companies. DGs connected to distribution networks have the potential to improve system voltage stability. In this study, the loadability limit is used as an index to security assessment [27]. The proposed index formulates and calculates as a nonlinear optimization problem. One of objectives of this study for the allocation DGs is maximizing the loadability limit, $P_T$, with the optimal placement of DGs. The system loadability limit can be evaluated by means of nonlinear optimization, in which it tries to maximize system loading under the constraint of power flow equations. For this purpose, the problem can be formulated as follows:

$$\begin{array}{ll} Min & : -P_T \\ s. & : \left\{ \begin{array}{l} P_{Gi} - P_{Di} - f_i(v,\delta) = 0 \\ Q_{Gi} - Q_{Di} - g_i(v,\delta) = 0 \end{array} \right. , \end{array} \tag{1}$$

where $P_T$ is the system total active load, $P_{Gi}$ and $Q_{Gi}$ represent vectors of active and reactive generation, $P_{Di}$ and $Q_{Di}$ represent vectors of active and reactive load, and $f_i$ and $g_i$ are active and reactive power flow equations, respectively.

The main constraint for voltage stability is the feasibility of the power flow solution; therefore, Eq. (1) tries to find maximum loading under the feasibility of the power flow equation, which corresponds to the system loadability limit. Eq. (1) can be solved using the Lagrange method. For this purpose, the nonconstrained Lagrange function can be constructed as follows:

$$L = -P_T + [\lambda]^T[P_G - P_D - f(V,\delta)] + [\gamma]^T[Q_G - Q_D - g(V,\delta)], \tag{2}$$

where $[\lambda]$ and $[\gamma]$ are vectors of Lagrange multipliers.

### 2.1.2. Model of load/generation increase

An increase of load and generation patterns at buses is one of the main factors that dominates the loadability limit; in order to include their effects, it can be modeled as shown below [27,28].

$$\begin{gathered} P_{Di} = \left[P_{Di}^{(0)} + \beta_i Pf_i(P_T - P_T^{(0)})\right]\left(\frac{V_i}{V_i^{(0)}}\right)^{kpvi} \\ Q_{Di} = \left[Q_{Di}^{(0)} + \beta_i Qf_i(Q_T - Q_T^{(0)})\right]\left(\frac{V_i}{V_i^{(0)}}\right)^{kqvi} \\ P_{Gi} = \alpha_i P_T \quad \alpha_i \le 1 \quad \sum_{i=2}^{NB} \beta_i = 1 \end{gathered} \tag{3}$$

$$Q_{Gi} = Q_{Gi}^{Max} \quad \sum_{i=2}^{NB} \alpha_i \leq 1 \tag{4}$$

Here, $P_{Di}^{(0)}$ and $Q_{Di}^{(0)}$ are the primary values of the active and reactive load powers, $\alpha_i$ and $\beta_i$ are the generation and load contributions for each bus, $Pf_i$ and $Qf_i$ are load factor coefficients, $V_i^0$ is the primary value of the bus voltage magnitude, $V_i$ is the value of the bus voltage, *kpvi* and *kqvi* are the load active and reactive powers, $P_T^{(0)}$ is the total primary active load of the system, and $P_T$ is the total active load of the system. Hence, the final Lagrange function will be as shown below.

$$\begin{aligned} L : & -\sum_{i=2}^{NB} \left[P_{Di}^{(0)} + \beta_i P f_i (P_T - P_T^{(0)})\right] \left(\frac{V_i}{V_i^{(0)}}\right)^{kpvi} + \\ & \sum_{i=2}^{NB} \lambda_i \left\{\alpha_i P_T - \left[P_{Di}^{(0)} + \beta_i P f_i (P_T - P_T^{(0)})\right] \left(\frac{V_i}{V_i^{(0)}}\right)^{kpvi} - f_i(v,\delta)\right\} + \\ & \sum_{i=2}^{NB} \gamma_i \left\{Q_{Gi}^{\max} - \left[Q_{Di}^{(0)} + \beta_i Q f_i (P_T - P_T^{(0)})\right] \left(\frac{V_i}{V_i^{(0)}}\right)^{kqvi} - g_i(v,\delta)\right\} \end{aligned} \tag{5}$$

For solving Eq. (5), the Newton-Raphson method is employed. For this purpose, the first derivatives of Eq. (5) are calculated as follows:

$$F_X = \frac{\partial L}{\partial X} = 0 \quad X = [V, \delta, \lambda, \gamma, P_T]\,. \tag{6}$$

The factors of each equation, which contain $\Delta V$, $\Delta\delta$, $\Delta\lambda$, $\Delta\gamma$, and $\Delta P_T$, are then calculated. By implementing Eq. (6), the following matrix can be obtained:

$$\begin{bmatrix} F_V^{(0)} \\ F_\delta^{(0)} \\ F_\lambda^{(0)} \\ F_\gamma^{(0)} \\ F_{P_T}^{(0)} \end{bmatrix} = \begin{bmatrix} F_{V\,V} & F_{V\,\delta} & F_{V\,\lambda} & F_{V\,\gamma} & F_{V\,P_T} \\ F_{\delta\,V} & F_{\delta\,\delta} & F_{\delta\,\lambda} & F_{\delta\,\gamma} & F_{\delta\,P_T} \\ F_{\lambda\,V} & F_{\lambda\,\delta} & F_{\lambda\,\lambda} & F_{\lambda\,\gamma} & F_{\lambda\,P_T} \\ F_{\gamma\,V} & F_{\gamma\,\delta} & F_{\gamma\,\lambda} & F_{\gamma\,\gamma} & F_{\gamma\,P_T} \\ F_{P_T\,V} & F_{P_T\,\delta} & F_{P_T\,\lambda} & F_{P_T\,\gamma} & F_{P_T\,P_T} \end{bmatrix} \begin{bmatrix} \Delta V \\ \Delta\delta \\ \Delta\lambda \\ \Delta\gamma \\ \Delta P_T \end{bmatrix}. \tag{7}$$

In this study, it is assumed that the first bus is a slack bus and, to simplify, it is assumed that all of the $PV$ buses are converted to $PQ$ in the maximum loadability limit condition ($Q_{G_i} = Q_i^{Max}$). This is based on the fact that in the maximum loadability condition, all of the capable reactive generations are generated.

It is noticeable that 3 models of $PV$ buses have been developed to reach the proper model of $PV$ buses in the developed voltage stability toolbox [27]. In the first model, a $PV$ bus is assumed as a $PQ$ bus, similar to this study with respect to the discussed reasons for the voltage collapse condition. This means that in the loadability limit condition, almost all of the $Q$ sources have been applied in the power network normally. The second proposed model is based on the model of $PV$ buses in a load flow problem. In the mentioned study, it was shown that this model is not proper for voltage stability studies. In the third model, the $PV$ bus is modeled with respect to the maximum exciting current of each generator ($I_{f\max}$), which is the proper and real model of $PV$ bus behavior in a voltage collapse condition. However, the proposed method has been implemented using MATLAB and, based on the described methodology, the voltage stability toolbox has been developed.

### 2.2. Power loss reduction index

One of the major potential benefits offered by DG is the reduction in electrical line losses. The loss can be significant under heavy load conditions. The utility is forced to pass the cost of electrical line losses to all customers by means of higher energy cost. With the inclusion of DG, line loss in the distribution system can be reduced. The proposed index for a bus is defined as follows:

$$\begin{aligned} O_2 &= \sum_{l=1}^{b} R_l I_l^2 = \\ &= \sum_{l=1}^{b} [V_i^2 + V_j^2 - 2V_iV_j\cos(\delta_i - \delta_j)]Y_{ij}\cos\varphi_{ij}, \end{aligned} \tag{8}$$

where $b$ is the number of branches, $R_l$ is the resistance of line $l$, $I_l$ is the current passing through line $l$, $V_i$ and $\delta_i$ are the voltage magnitude and voltage angle of node $I$, and $Y_{ij}$ and $\varphi_{ij}$ are the magnitude and angle of the $i-j$ line admittance.

Hence, the objective function includes 2 terms that maximize the voltage stability margin and minimize the power losses in DG allocation. This will be described more in detail in the next sections.

## 3. PSO and HPSO algorithms

### 3.1. Brief survey

In this section, we discuss the main topic, which is an introduction on hybrid algorithms, of which PSO is one of the prime algorithms. A natural evolution of the population-based search algorithms, like that of PSO, can be achieved by integrating the methods that have already been tested successfully for solving complex problems. Researchers have enhanced the performance of PSO by incorporating in it the fundamentals of other popular techniques like selection, mutation, and a crossover of the GA and differential evolution (DE) algorithms. Moreover, attempts have been made to improve the performance of other evolutionary algorithms like GA, DE, and ant colony optimization (ACO) by integrating into them the velocity and position update equations of PSO. The main goal, as we see it, is to harness the strong points of the algorithms in order to keep a balance between the exploration and exploitation factors, thereby preventing the stagnation of the population and preventing premature convergence.

In a PSO system, multiple candidate solutions coexist and collaborate simultaneously. Each solution candidate, called a "particle", flies in the problem space looking for the optimal position. A particle with time adjusts its position to its own experience, while adjusting to the experience of neighboring particles. If a particle discovers a promising new solution, all of the other particles will move closer to it, exploring the region more thoroughly in the process. This new approach features many advantages. First of all, PSO is very simple, easy to understand, and a natural algorithm. It is fast and can be coded in a few lines. Moreover, its strength requirement is minimal [31-34]. Despite the passage of more than a decade, this algorithm still has many noted researchers. The debut of the PSO algorithm took place in 1995 with the first paper by Kennedy and Eberhart [35]. Recently in [36], Li et al. proposed a hybrid of PSO and GA called the PSOGA-based hybrid algorithm (PGHA) for optimization design. They used improved genetic mechanisms like nonlinear ranking selection for the GA process. They generated 3 offspring from 2 parents and used a newly defined mutation operator. Ting et al. [37] proposed a hybrid constrained GA/PSO algorithm for solving load flow problems. Jeong et al. [38]

proposed a hybrid algorithm called the GA/PSO for solving multiobjective optimization problems, and they validated their algorithm on test problems and also on engineering design problems. In this algorithm, the first multiple solutions are generated randomly as an initial population and objective function values are evaluated for each solution. After the evaluation, the population is divided into 2 subpopulations, one of which is updated by the GA operation, while the other is updated by PSO operation. Kannan et al. used the combination of fuzzy and HPSO methods for optimal allocation of capacitors in a power network [23]. Valdez et al. integrated the concept of fuzzy logic into a hybrid of the GA and PSO algorithm [39]. The new hybrid algorithm, called PSO + GA, also works by dividing the individuals into GA and PSO populations. However, it differs from the previous approaches as the GA + PSO fuzzy rules are applied to decide whether to take GA individuals or to take PSO individuals. Bhuvaneswari et al. [40] reported a hybrid approach using GA and PSO called hybrid genetic algorithm-particle swarm optimization (HGAPSO). Abdel-Kader [41] proposed the genetically improved particle swarm optimization (GAI-PSO) algorithm, which combines the standard velocity and position update rules of PSO with the ideas of selection and crossover from GAs. The GAI-PSO algorithm searches the solution space to find the optimal initial cluster centroids for the next phase. The second phase is a local refining stage, utilizing the k-means algorithm, which can efficiently converge to the optimal solution. The proposed algorithm combines the ability of globalized searching of the evolutionary algorithms and the fast convergence of the k-means algorithm, and it can avoid the drawbacks of both.

It is clear that HPSO is a powerful optimization technique that has been applied to a wide range of optimization problems. Nevertheless, its performance can be enhanced many-fold with the aid of certain modifications. The present research article focuses on the concept of hybridization, which is presently a popular idea being applied to evolutionary algorithms in order to increase

their efficiency and robustness. In this paper we use this algorithm to solve the modeled optimization problem.

## 3.2. Definition

The PSO definition is presented as follows:

1) Each individual particle $i$ has the following properties:

$x_i$, $v_i$: current position and velocity in the search space,

$y_i$: personal best position in the search space.

2) The personal best position, $p_i$, corresponds to the position in the search space where particle $i$ presents the smallest error as determined by objective function $f$, assuming a minimization task.

3) The global best position denoted by $g$ represents the position yielding the lowest error among all $p_i$s.

Eqs. (9) and (10) define how the personal and global best values are updated at time k, respectively. Below, it is assumed that the swarm consists of $s$ particles [18,19].

Thus, $i$ E 1, . . . , $s$:

$$p_i^{k+1} = \begin{cases} p_i^k & \text{if} \quad f\left(p_i^k\right) \leq f\left(X_i^{k+1}\right) \\ X_i^{k+1} & \text{if} \quad f\left(p_i^k\right) > f\left(X_i^{k+1}\right) \end{cases}, \tag{9}$$

$$\begin{array}{l} g^k \in \left\{p_1^k, p_2^k, ..., p_S^k\right\} \\ f\left(g^k\right) = \min\left\{f\left(p_1^k\right), f\left(p_2^k\right), ..., f\left(p_S^k\right)\right\} \end{array}. \tag{10}$$

During each iteration, every particle in the swarm is updated using Eqs. (11) and (12). Two pseudorandom sequences, $r1 \sim U(0,1)$ and $r2 \sim U(0,1)$, are used to affect the stochastic nature of the algorithm.

$$v_i^{k+1} = w \times v_i^k + c_1 \times rand()_1 \times \left(p_i^k - X_i^k\right) + c_2 \times rand()_2 \times \left(g^k - X_i^k\right) \tag{11}$$

$$X_i^{k+1} = X_i^k + v_i^{k+1} \tag{12}$$

$$w = w_{\max} - \frac{w_{\max} - w_{\max}}{iter_{\max}} \times iter \tag{13}$$

$$v_{\max} = k \times x_{\max} \quad 0.1 \le k \le 1 \tag{14}$$

Here, $v_i^k$ is the velocity of the $i$th particle at the $k$th iteration; $v_i^{k+1}$ is the velocity of the $i$th particle at the $(k+1)$th iteration; $w$ is the inertia weight; $X_i^k$ is the position of the $i$th particle at the $k$th iteration; $X_i^{k+1}$ is the position of the $i$th particle at the $(k+1)$th iteration; $c_1$ and $c_2$ are positive constants both equal to 2; *iter* and $iter_{max}$ are the iteration number and maximum iteration number; and $rand()_1$ and $rand()_2$ are random numbers selected between 0 and 1.

Evolutionary operators like selection, crossover, and mutation have been applied to PSO. By applying the selection operation in PSO, the particles with the best performance are copied into the next generation; therefore, PSO can always keep the best performed particles. By applying the crossover operation, information can be exchanged or swapped between 2 particles so that they can “fly” to the new search area as in evolutionary programming and GAs. Among the 3 evolutionary operators, the mutation operators are the most commonly applied evolutionary operators in PSO. The purpose of applying mutation to PSO is to increase the diversity of the population and the ability to have the PSO escape the local minima. HPSO uses the mechanism of PSO and a natural selection mechanism utilizing the GA [18,29].

# 4. Implementation HPSO algorithm

## 4.1. Initialization

In this study, the optimum values of the parameters are easily and accurately computed using the HPSO. In a typical run of the HPSO, an initial population is randomly generated. This initial population is referred to as the 0th generation. Each individual in the initial population has an associated performance index value. Using the performance index information, the HPSO then produces a new population. In order to obtain the value of the performance index for each of the individuals in the current population, the system must be simulated. The HPSO then produces the next generation of individuals using the reproduction crossover and mutation operators. These processes are repeated until the population is converged and the optimum value of the parameters is found. Each designed chromosome is a 5-component vector. These components represent the locations and the nodes in which the DGs should be connected, and they can take values from 2 to the number of buses in the network. A population of possible solutions will evolve from one generation to another, in order to obtain a very well fitted individual.

## 4.2. Fitness function

This function measures the quality of each chromosome of populations and it is closely related to the objective function. The objective function is computed using Eqs. (1)-(8). In this study, 1 generation and 4 load pattern scenarios are considered. Hence, in each iteration, 4 objective functions values are calculated by Eq. (15), and the fitness value is calculated by means of these 4 values by Eq. (16). The effects of DG on maximizing the loadability limit and minimizing power losses are considered in this section with its contribution of the generation pattern in the power system. The contribution of the generation of each DG is added to the contribution of the generation of each bus at which algorithms place the DGs, and the $P_T$ and power losses are calculated. Corresponding coefficients are used for each objective. The overall objective function designed during this study is:

$$f_i(x) = K_1.P_{T_i} - K_2.\,P_{Loss_i}, \tag{15}$$

where $K_1$ and $K_2$ are arbitrary gain factors. They imply a tradeoff between security and losses. Their values are 10% and 90%, respectively, in the simulation studies, as well.

Based on the scenarios (generations and loads patterns), the final fitness value is calculated by the means of these 4 values:

$$F(x) = \frac{\sum_{i=1}^{4} f_i(x)}{K_S}, \tag{16}$$

where $K_S$ is the number of patterns, which is 4 in this study.

## 5. Case study

The IEEE 14-bus, 220 kV, and IEEE 30-bus are used as test systems. The single line diagrams of these systems are shown in Figures 1 and 2. The IEEE 14-bus network consists of 5 generators, 11 consumers, and 15 interconnected lines (Table 1). DG units are applied to $PQ$ buses based on their contributions in real power generation (Figure 3). The IEEE 30-bus network consists of 6 generators, 22 consumers, and 41 interconnected lines (Table 2).

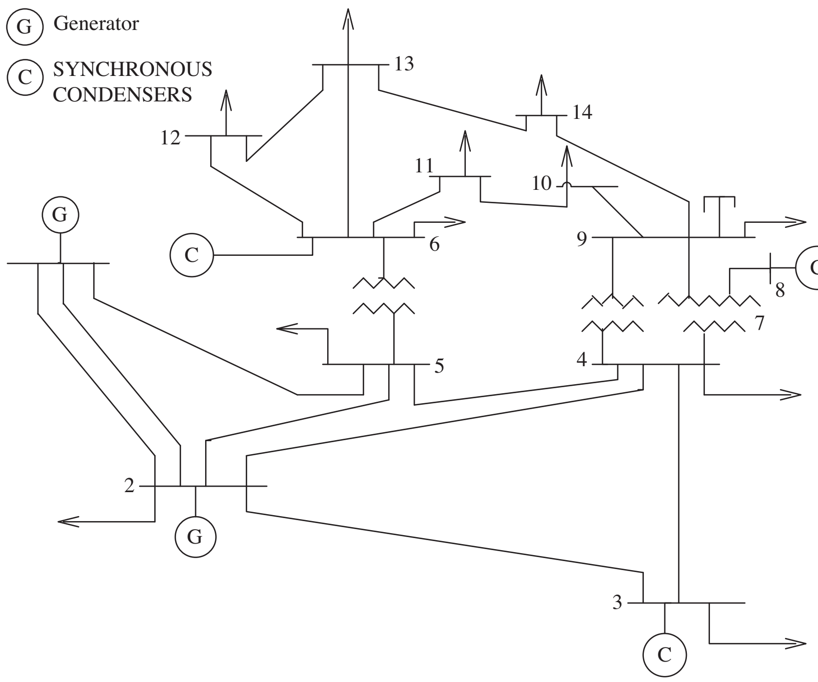


**Figure 1.** Single-line diagram of the IEEE 14-bus test network.

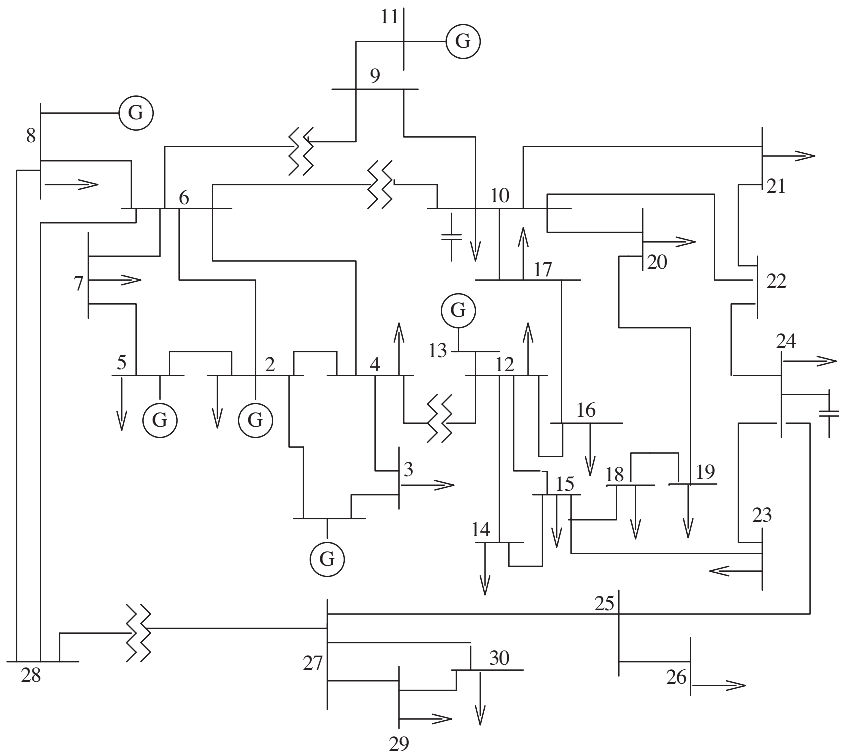


**Figure 2.** Single-line diagram of the IEEE 30-bus test network.

**Table 1.** Line data for the IEEE 14-bus system.

| From | To | R(p.u) | X(p.u) | B | Tap |
|---|---|---|---|---|---|
| **1** | **2** | 0.01938 | 0.05917 | 0.0528 | 1 |
| **1** | **5** | 0.05403 | 0.22304 | 0.0492 | 1 |
| **2** | **3** | 0.04699 | 0.19797 | 0.0438 | 1 |
| **2** | **4** | 0.05811 | 0.17632 | 0.0374 | 1 |
| **2** | **5** | 0.05695 | 0.17388 | 0.0340 | 1 |
| **3** | **4** | 0.06701 | 0.17103 | 0.0346 | 1 |
| **4** | **5** | 0.01335 | 0.04211 | 0.0128 | 1 |
| **6** | **11** | 0.09498 | 0.1989 | 0.0000 | 1 |
| **6** | **12** | 0.12291 | 0.25581 | 0.0000 | 1 |
| **6** | **13** | 0.06615 | 0.13027 | 0.0000 | 1 |
| **7** | **8** | 0.00000 | 0.17615 | 0.0000 | 1 |
| **7** | **9** | 0.00000 | 0.11010 | 0.0000 | 1 |
| **9** | **10** | 0.03181 | 0.08450 | 0.0000 | 1 |
| **9** | **14** | 0.12711 | 0.27038 | 0.0000 | 1 |
| **10** | **11** | 0.08205 | 0.19207 | 0.0000 | 1 |
| **12** | **13** | 0.22092 | 0.19988 | 0.0000 | 1 |
| **13** | **14** | 0.17093 | 0.34802 | 0.0000 | 1 |
| **4** | **7** | 0.00000 | 0.20912 | 0.0000 | 0.978 |
| **4** | **9** | 0.00000 | 0.55618 | 0.0000 | 0.969 |
| **5** | **6** | 0.00000 | 0.25202 | 0.0000 | 0.932 |

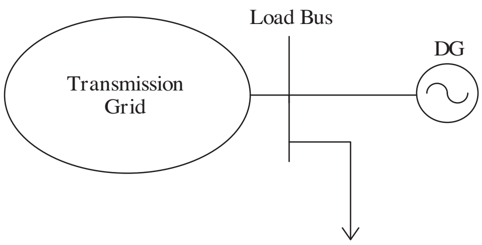


**Figure 3.** System model with the connection of a DG unit.

**Table 2.** Line data for the IEEE 30-bus system.

| No. line | From | To | R(p.u) | X(p.u) | B | Tap | No. line | From | To | R(p.u) | X(p.u) | B | Tap |
|---|---|---|---|---|---|---|---|---|---|---|---|---|---|
| **1** | 1 | 2 | 0.0192 | 0.0575 | 0.0528 | 1 | **22** | 10 | 20 | 0.0936 | 0.209 | 0.0000 | 1 |
| **2** | 1 | 3 | 0.0452 | 0.1852 | 0.0408 | 1 | **23** | 10 | 17 | 0.0324 | 0.0845 | 0.0000 | 1 |
| **3** | 2 | 4 | 0.0507 | 0.1737 | 0.0368 | 1 | **24** | 10 | 21 | 0.0348 | 0.0749 | 0.0000 | 1 |
| **4** | 3 | 4 | 0.0132 | 0.0379 | 0.0084 | 1 | **25** | 10 | 22 | 0.0727 | 0.1499 | 0.0000 | 1 |
| **5** | 2 | 5 | 0.0472 | 0.1983 | 0.0418 | 1 | **26** | 21 | 22 | 0.0116 | 0.0236 | 0.0000 | 1 |
| **6** | 2 | 6 | 0.0581 | 0.1763 | 0.0374 | 1 | **27** | 15 | 23 | 0.1000 | 0.202 | 0.0000 | 1 |
| **7** | 4 | 6 | 0.0119 | 0.0414 | 0.009 | 1 | **28** | 22 | 24 | 0.115 | 0.179 | 0.0000 | 1 |
| **8** | 5 | 7 | 0.046 | 0.116 | 0.0204 | 1 | **29** | 23 | 24 | 0.132 | 0.27 | 0.0000 | 1 |
| **9** | 6 | 7 | 0.0267 | 0.082 | 0.017 | 1 | **30** | 24 | 25 | 0.1885 | 0.3292 | 0.0000 | 1 |
| **10** | 6 | 8 | 0.012 | 0.042 | 0.009 | 1 | **31** | 25 | 26 | 0.2544 | 0. 38 | 0.0000 | 1 |
| **11** | 9 | 11 | 0.00000 | 0.208 | 0.0000 | 1 | **32** | 25 | 27 | 0.1093 | 0.2087 | 0.0000 | 1 |
| **12** | 9 | 10 | 0.00000 | 0.11 | 0.0000 | 1 | **33** | 27 | 29 | 0.2198 | 0.4153 | 0.0000 | 1 |
| **13** | 12 | 13 | 0.00000 | 0.14 | 0.0000 | 1 | **34** | 27 | 30 | 0.3202 | 0.6027 | 0.0000 | 1 |
| **14** | 12 | 14 | 0.1231 | 0.2559 | 0.0000 | 1 | **35** | 29 | 30 | 0.2399 | 0.4533 | 0.0000 | 1 |
| **15** | 12 | 15 | 0.0662 | 0.1304 | 0.0000 | 1 | **36** | 8 | 28 | 0.0636 | 0.2 | 0.0428 | 1 |
| **16** | 12 | 16 | 0.0945 | 0.1987 | 0.0000 | 1 | **37** | 6 | 28 | 0.0169 | 0.0599 | 0.012 | 1 |
| **17** | 14 | 15 | 0.221 | 0.1997 | 0.0000 | 1 | **38** | 6 | 9 | 0.0000 | 0.208 | 0.0000 | 1.0155 |
| **18** | 16 | 17 | 0.0824 | 0.1932 | 0.0000 | 1 | **39** | 6 | 10 | 0.0000 | 0.556 | 0.0000 | 0.9629 |
| **19** | 15 | 18 | 0.107 | 0.2185 | 0.0000 | 1 | **40** | 4 | 12 | 0.0000 | 0.256 | 0.0000 | 1.0129 |
| **20** | 18 | 19 | 0.0639 | 0.1292 | 0.0000 | 1 | **41** | 26 | 27 | 0.0000 | 0.396 | 0.0000 | 0.9581 |
| **21** | 19 | 20 | 0.034 | 0.068 | 0.0000 | 1 | | | | | | | |

One generation and 4 load patterns are considered in this paper to involve a real operational power network. Their data are given in Tables 3 and 4. In each of the algorithm's iterations, 4 objective values are calculated, respectively, from 1 generation and 4 load patterns, and by means of these values, the fitness of each population is calculated. This creates all of the scenarios for load increasing and generation scheduling mentioned in this study. Hence, the load and generation effects are applied in optimal DG placement. The program is run without DG placement and the results for the total network power losses and loadability limit are derived, as in Table 5.

Five DGs (1.5, 0.78, 0.78, 6, and 3.2 MW) are considered for placement on 5 buses in the power systems for improving the voltage stability index, $P_T$, and minimizing power losses. The results of the mentioned algorithms for 5 running times are summarized in Tables 6-9. These results show that the proposed algorithms suggested weak buses for optimal DG placement. Moreover, it causes an improvement in the loadability limit of system and voltage magnitudes, and a reduction in total power losses. The initial population is randomly generated.

**Table 3.** Generation and load patterns (14-bus).

| Bus | $\alpha_1$ | $\beta_1$ | $\beta_2$ | $\beta_3$ | $\beta_4$ |
|---|---|---|---|---|---|
| **1** | 0.00 | 0.00 | 0.00 | 0.00 | 0.00 |
| **2** | 0.14052 | 0.084 | 0.08 | 0.083 | 0.085 |
| **3** | 0.00 | 0.364 | 0.368 | 0.362 | 0.36 |
| **4** | 0.00 | 0.185 | 0.18 | 0.1951 | 0.187 |
| **5** | 0.00 | 0.0293 | 0.0298 | 0.0299 | 0.029 |
| **6** | 0.00 | 0.0432 | 0.0475 | 0.0463 | 0.0414 |
| **7** | 0.00 | 0.00 | 0.00 | 0.00 | 0.00 |
| **8** | 0.00 | 0.00 | 0.00 | 0.00 | 0.00 |
| **9** | 0.00 | 0.1132 | 0.11 | 0.1123 | 0.102 |
| **10** | 0.00 | 0.0347 | 0.0342 | 0.035 | 0.0244 |
| **11** | 0.00 | 0.0135 | 0.0142 | 0.014 | 0.024 |
| **12** | 0.00 | 0.0235 | 0.0262 | 0.0282 | 0.026 |
| **13** | 0.00 | 0.0521 | 0.0531 | 0.0534 | 0.0639 |
| **14** | 0.00 | 0.0575 | 0.057 | 0.0408 | 0.0573 |

**Table 4.** Generation and load patterns (30-bus).

| Bus No. | $\alpha_1$ | $\beta_1$ | $\beta_2$ | $\beta_3$ | $\beta_4$ | Bus No. | $\alpha_1$ | $\beta_1$ | $\beta_2$ | $\beta_3$ | $\beta_4$ |
|---|---|---|---|---|---|---|---|---|---|---|---|
| **1** | 0.4572 | 0.00 | 0.00 | 0.00 | 0.00 | **16** | 0.00 | 0.0012 | 0.0002 | 0.0032 | 0.003 |
| **2** | 0.1902 | 0.08 | 0.07 | 0.06 | 0.068 | **17** | 0.00 | 0.032 | 0.033 | 0.03 | 0.0302 |
| **3** | 0.00 | 0.008 | 0.018 | 0.028 | 0.02 | **18** | 0.00 | 0.011 | 0.022 | 0.033 | 0.03 |
| **4** | 0.00 | 0.027 | 0.017 | 0.01 | 0.012 | **19** | 0.00 | 0.033 | 0.022 | 0.011 | 0.012 |
| **5** | 0.0816 | 0.33 | 0.34 | 0.3529 | 0.35 | **20** | 0.00 | 0.007 | 0.004 | 0.014 | 0.015 |
| **6** | 0.00 | 0.00 | 0.00 | 0.00 | 0.00 | **21** | 0.00 | 0.061 | 0.064 | 0.054 | 0.055 |
| **7** | 0.00 | 0.08 | 0.06 | 0.16 | 0.1109 | **22** | 0.00 | 0.00 | 0.00 | 0.00 | 0.00 |
| **8** | 0.1162 | 0.1 | 0.12 | 0.02 | 0.03 | **23** | 0.00 | 0.0011 | 0.001 | 0.021 | 0.01 |
| **9** | 0.00 | 0.00 | 0.00 | 0.00 | 0.00 | **24** | 0.00 | 0.03 | 0.0301 | 0.0101 | 0.0111 |
| **10** | 0.00 | 0.02 | 0.03 | 0.04 | 0.05 | **25** | 0.00 | 0.00 | 0.00 | 0.00 | 0.00 |
| **11** | 0.0595 | 0.00 | 0.00 | 0.00 | 0.00 | **26** | 0.00 | 0.0123 | 0.0195 | 0.01353 | 0.023 |
| **12** | 0.00 | 0.04 | 0.03 | 0.02 | 0.03 | **27** | 0.00 | 0.00 | 0.00 | 0.00 | 0.00 |
| **13** | 0.0557 | 0.00 | 0.00 | 0.00 | 0.00 | **28** | 0.00 | 0.00 | 0.00 | 0.00 | 0.00 |
| **14** | 0.00 | 0.02 | 0.03 | 0.04 | 0.05 | **29** | 0.00 | 0.008 | 0.0088 | 0.00844 | 0.0089 |
| **15** | 0.00 | 0.03 | 0.02 | 0.01 | 0.02 | **30** | 0.00 | 0.0684 | 0.0604 | 0.06083 | 0.0609 |

**Table 5.** The results without DG placement.

| 14-bus system | | 30-bus system | |
|---|---|---|---|
| $P_T$ (MW) | $P_{loss}$(MW) | $P_T$ (MW) | $P_{loss}$(MW) |
| 447.92 | 83.07 | 301.26 | 24.08 |

Figures 4 and 5 show the performances of the algorithms for first runs. The graphs show a good convergence of the fitness value with the generations. The best fitness value rises with generations, which shows that these algorithms are suitable for solving the DG optimal location problem. With respect to the mentioned graphs, the HPSO algorithm has better performance compared with the other algorithm, since its converging graph has better and faster convergence behavior than that of PSO. It is obvious that the HPSO algorithm has a proper convergence in low iteration numbers because the HPSO algorithm converges in the 5th-6th iteration. Moreover, the main object of this paper is maximizing the fitness function, and the convergence graph of HPSO shows better results when compared to PSO.

**Table 6.** Best population for each running time of PSO for the IEEE 14-bus system.

| Run Iter | Bus No. 1 | Bus No. 2 | Bus No. 3 | Bus No. 4 | Bus No. 5 | $P_T$(MW) | $P_{loss}$(MW) |
|---|---|---|---|---|---|---|---|
| **1st** | 3 | 3 | 3 | 3 | 3 | 455.6 | 80.64 |
| **2nd** | 3 | 9 | 8 | 3 | 3 | 456.43 | 80.92 |
| **3rd** | 3 | 8 | 3 | 3 | 3 | 455.83 | 80.84 |
| **4th** | 3 | 8 | 3 | 3 | 3 | 455.83 | 80.84 |
| **5th** | 3 | 3 | 3 | 3 | 3 | 455.6 | 80.64 |

**Table 7.** Best population for each running time of HPSO for the IEEE 14-bus system.

| Run Iter | Bus No. 1 | Bus No. 2 | Bus No. 3 | Bus No. 4 | Bus No. 5 | $P_T$(MW) | $P_{loss}$(MW) |
|---|---|---|---|---|---|---|---|
| **1st** | 3 | 3 | 3 | 3 | 3 | 455.94 | 80.45 |
| **2nd** | 8 | 8 | 3 | 3 | 3 | 456.32 | 80.93 |
| **3rd** | 3 | 3 | 3 | 3 | 3 | 455.94 | 80.45 |
| **4th** | 3 | 14 | 3 | 3 | 3 | 456.56 | 80.86 |
| **5th** | 3 | 3 | 3 | 3 | 3 | 455.94 | 80.45 |

**Table 8.** Best population for each running time of PSO for the IEEE 30-bus system.

| Run Iter | Bus No. 1 | Bus No. 2 | Bus No. 3 | Bus No. 4 | Bus No. 5 | $P_T$(MW) | $P_{loss}$(MW) |
|---|---|---|---|---|---|---|---|
| **1st** | 5 | 29 | 29 | 30 | 29 | 332.72 | 22.5 |
| **2nd** | 26 | 15 | 5 | 29 | 29 | 329.81 | 22.15 |
| **3rd** | 5 | 29 | 8 | 29 | 29 | 325.69 | 21.61 |
| **4th** | 26 | 29 | 8 | 30 | 5 | 323.21 | 21.51 |
| **5th** | 5 | 30 | 18 | 30 | 29 | 334.88 | 22.84 |

**Table 9.** Best population for each running time of HPSO for the IEEE 30-bus system.

| Run Iter | Bus No. 1 | Bus No. 2 | Bus No. 3 | Bus No. 4 | Bus No. 5 | $P_T$(MW) | $P_{loss}$(MW) |
|---|---|---|---|---|---|---|---|
| **1st** | 11 | 11 | 30 | 30 | 30 | 334.93 | 22.78 |
| **2nd** | 11 | 30 | 30 | 30 | 30 | 337.31 | 22.98 |
| **3rd** | 30 | 2 | 30 | 30 | 30 | 339.45 | 23.21 |
| **4th** | 30 | 30 | 30 | 30 | 30 | 341.86 | 23.39 |
| **5th** | 30 | 11 | 30 | 30 | 30 | 339.5 | 23.18 |

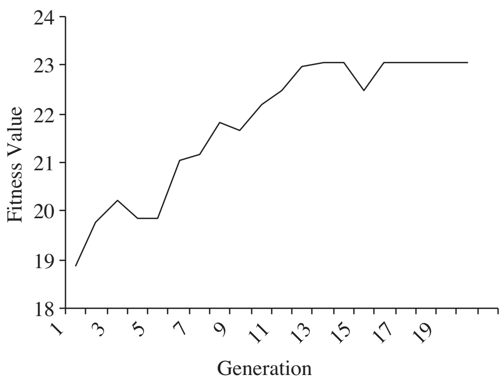


**Figure 4.** PSO performance for the 1st run (14-bus).

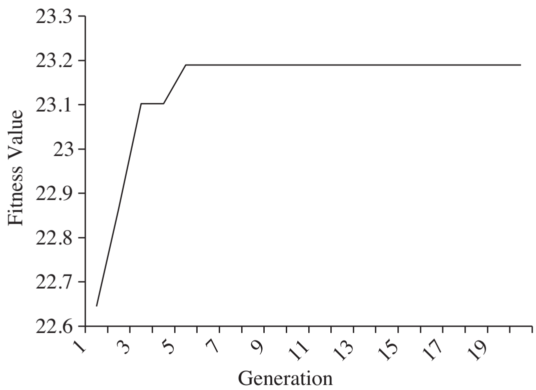


**Figure 5.** HPSO performance for the 1st run (14-bus).

Tables 10 and 11 show the results of the bus voltage magnitude and maximum loading of each bus for executing the program in a voltage collapse condition without installing DGs.

**Table 10.** Bus loading and voltage without DG placement for the IEEE 14-bus system.

| Bus No. | $V_{pre-install}\,(p.u)$ | $P_{max-pre-install}\,(MW)$ | Bus No. | $V_{pre-install}\,(p.u)$ | $P_{max-pre-install}\,(MW)$ |
|---|---|---|---|---|---|
| **1** | 1.06 | 0.00 | **8** | 0.7743 | 0.00 |
| **2** | 0.8951 | 37.26 | **9** | 0.674 | 49.1 |
| **3** | 0.738 | 163.17 | **10** | 0.661 | 14.4 |
| **4** | 0.7463 | 83.86 | **11** | 0.6751 | 7.37 |
| **5** | 0.7741 | 13.24 | **12** | 0.6672 | 11.66 |
| **6** | 0.7123 | 20.02 | **13** | 0.6544 | 24.97 |
| **7** | 0.7197 | 0.00 | **14** | 0.6155 | 23.84 |

**Table 11.** Bus loading and voltage without DG placement for the IEEE 30-bus system.

| Bus No. | $V_{pre-install}\,(p.u)$ | $P_{max-pre-install}\,(MW)$ | Bus No. | $V_{pre-install}\,(p.u)$ | $P_{max-pre-install}\,(MW)$ |
|---|---|---|---|---|---|
| **1** | 1.0600 | 0 | **16** | 0.9889 | 0.58 |
| **2** | 1.0339 | 20.86 | **17** | 0.9790 | 9.43 |
| **3** | 1.0258 | 5.62 | **18** | 0.9575 | 7.27 |
| **4** | 1.0185 | 4.94 | **19** | 0.9597 | 5.84 |
| **5** | 0.9943 | 103.44 | **20** | 0.9644 | 3.02 |
| **6** | 1.0153 | 0 | **21** | 0.9570 | 17.61 |
| **7** | 0.9954 | 31.16 | **22** | 0.9535 | 0 |
| **8** | 1.0268 | 20.18 | **23** | 0.9274 | 2.54 |
| **9** | 1.0015 | 0 | **24** | 0.8833 | 6.09 |
| **10** | 0.9833 | 10.56 | **25** | 0.7287 | 0 |
| **11** | 1.0427 | 0 | **26** | 0.6598 | 5.13 |
| **12** | 1.0011 | 8.99 | **27** | 0.6744 | 0 |
| **13** | 1.0386 | 0 | **28** | 1.0192 | 0 |
| **14** | 0.9741 | 10.56 | **29** | 0.6173 | 2.57 |
| **15** | 0.9668 | 5.98 | **30** | 0.5766 | 18.85 |

Tables 12-14 show the magnitude of bus voltages of each bus in the network with the placement of the 5 mentioned DGs. Tables 13-15 show the increase in the maximum loading of each bus in network with the placement of the 5 mentioned DGs. These tables show that with the placement of DGs on the proposed buses, bus voltage magnitude and maximum bus loading improve in almost all of the buses. With comparison results between the 2 algorithms, it is obvious that the HPSO results proposed better choices than those of the PSO algorithm.

**Table 12.** Bus voltage in 5 time runs for the IEEE 14-bus system.

| Bus No. | $V_{after-install-DG}$ | | | | | | | | | |
|---|---|---|---|---|---|---|---|---|---|---|
| | PSO runs | | | | | HPSO runs | | | | |
| | *# 1* | *# 2* | *# 3* | *# 4* | *# 5* | *# 1* | *# 2* | *# 3* | *# 4* | *# 5* |
| **1** | 1.0600 | 1.0600 | 1.0600 | 1.0600 | 1.0600 | 1.0600 | 1.0600 | 1.0600 | 1.0600 | 1.0600 |
| **2** | 0.8982 | 0.8979 | 0.8978 | 0.8982 | 0.8982 | 0.8986 | 0.8979 | 0.8986 | 0.8979 | 0.8986 |
| **3** | 0.7461 | 0.7463 | 0.7441 | 0.7467 | 0.7461 | 0.7483 | 0.7460 | 0.7483 | 0.7465 | 0.7483 |
| **4** | 0.7494 | 0.7488 | 0.7488 | 0.7488 | 0.7494 | 0.7493 | 0.7490 | 0.7493 | 0.7484 | 0.7493 |
| **5** | 0.7765 | 0.7760 | 0.7761 | 0.7762 | 0.7765 | 0.7764 | 0.7762 | 0.7764 | 0.7756 | 0.7764 |
| **6** | 0.7115 | 0.7106 | 0.7117 | 0.7112 | 0.7115 | 0.7110 | 0.7108 | 0.7110 | 0.7103 | 0.7110 |
| **7** | 0.7202 | 0.7197 | 0.7202 | 0.7196 | 0.7202 | 0.7198 | 0.7200 | 0.7198 | 0.7191 | 0.7198 |
| **8** | 0.7747 | 0.7743 | 0.7748 | 0.7742 | 0.7747 | 0.7744 | 0.7745 | 0.7744 | 0.7737 | 0.7744 |
| **9** | 0.6735 | 0.6729 | 0.6737 | 0.6728 | 0.6735 | 0.6730 | 0.6731 | 0.6730 | 0.6723 | 0.6730 |
| **10** | 0.6601 | 0.6598 | 0.6604 | 0.6595 | 0.6601 | 0.6596 | 0.6597 | 0.6596 | 0.6588 | 0.6596 |
| **11** | 0.6740 | 0.6734 | 0.6743 | 0.6736 | 0.6740 | 0.6735 | 0.6735 | 0.6735 | 0.6728 | 0.6735 |
| **12** | 0.6655 | 0.6645 | 0.6659 | 0.6652 | 0.6655 | 0.6649 | 0.6647 | 0.6649 | 0.6643 | 0.6649 |
| **13** | 0.6526 | 0.6516 | 0.6530 | 0.6523 | 0.6526 | 0.6520 | 0.6519 | 0.6520 | 0.6515 | 0.6520 |
| **14** | 0.6135 | 0.6125 | 0.6139 | 0.6128 | 0.6135 | 0.6128 | 0.6128 | 0.6128 | 0.6131 | 0.6128 |

**Table 13.** Bus loadings in 5 time runs for the IEEE 14-bus system.

| Bus No. | $V_{after-install-DG}$ | | | | | | | | | |
|---|---|---|---|---|---|---|---|---|---|---|
| | PSO runs | | | | | HPSO runs | | | | |
| | *# 1* | *# 2* | *# 3* | *# 4* | *# 5* | *# 1* | *# 2* | *# 3* | *# 4* | *# 5* |
| **1** | 0 | 0 | 0 | 0 | 0 | 0 | 0 | 0 | 0 | 0 |
| **2** | 37.82 | 37.89 | 37.73 | 37.84 | 37.82 | 37.85 | 37.88 | 37.85 | 37.90 | 37.85 |
| **3** | 165.61 | 165.91 | 165.21 | 165.69 | 165.61 | 165.73 | 165.87 | 165.73 | 165.95 | 165.73 |
| **4** | 85.11 | 85.27 | 84.91 | 85.16 | 85.11 | 85.18 | 85.25 | 85.18 | 85.29 | 85.18 |
| **5** | 13.44 | 13.47 | 13.41 | 13.45 | 13.44 | 13.45 | 13.46 | 13.45 | 13.47 | 13.45 |
| **6** | 20.32 | 20.36 | 20.27 | 20.33 | 20.32 | 20.34 | 20.35 | 20.34 | 20.36 | 20.34 |
| **7** | 0 | 0 | 0 | 0 | 0 | 0 | 0 | 0 | 0 | 0 |
| **8** | 0 | 0 | 0 | 0 | 0 | 0 | 0 | 0 | 0 | 0 |
| **9** | 49.83 | 49.93 | 49.72 | 49.86 | 49.83 | 49.87 | 49.91 | 49.87 | 49.94 | 49.87 |
| **10** | 14.62 | 14.64 | 14.58 | 14.62 | 14.62 | 14.63 | 14.64 | 14.63 | 14.65 | 14.63 |
| **11** | 7.48 | 7.50 | 7.46 | 7.49 | 7.48 | 7.49 | 7.49 | 7.49 | 7.50 | 7.49 |
| **12** | 11.84 | 11.86 | 11.81 | 11.84 | 11.84 | 11.85 | 11.86 | 11.85 | 11.86 | 11.85 |
| **13** | 25.34 | 25.39 | 25.28 | 25.35 | 25.34 | 25.36 | 25.38 | 25.36 | 25.40 | 25.36 |
| **14** | 24.19 | 24.24 | 24.14 | 24.21 | 24.19 | 24.21 | 24.23 | 24.21 | 24.25 | 24.21 |

**Table 14.** Bus voltage in 5 time runs for the IEEE 30-bus system.

| Bus No. | $V_{after-install-DG}$ | | | | | | | | | |
|---|---|---|---|---|---|---|---|---|---|---|
| | PSO runs | | | | | HPSO runs | | | | |
| | # 1 | # 2 | # 3 | # 4 | # 5 | # 1 | # 2 | # 3 | # 4 | # 5 |
| **1** | 1.0600 | 1.0600 | 1.0600 | 1.0600 | 1.0600 | 1.0600 | 1.0600 | 1.0600 | 1.0600 | 1.0600 |
| **2** | 1.0254 | 1.0267 | 1.0285 | 1.0294 | 1.0246 | 1.0247 | 1.0237 | 1.0228 | 1.0219 | 1.0229 |
| **3** | 1.0141 | 1.0159 | 1.0183 | 1.0193 | 1.0130 | 1.0130 | 1.0117 | 1.0103 | 1.0091 | 1.0105 |
| **4** | 1.0046 | 1.0068 | 1.0097 | 1.0108 | 1.0034 | 1.0033 | 1.0018 | 1.0001 | 0.9988 | 1.0003 |
| **5** | 0.9746 | 0.9776 | 0.9816 | 0.9839 | 0.9730 | 0.9730 | 0.9711 | 0.9691 | 0.9673 | 0.9692 |
| **6** | 0.9996 | 1.0020 | 1.0054 | 1.0066 | 0.9981 | 0.9982 | 0.9964 | 0.9946 | 0.9930 | 0.9948 |
| **7** | 0.9763 | 0.9792 | 0.9830 | 0.9848 | 0.9747 | 0.9747 | 0.9728 | 0.9707 | 0.9689 | 0.9709 |
| **8** | 1.0114 | 1.0138 | 1.0172 | 1.0183 | 1.0099 | 1.0100 | 1.0083 | 1.0064 | 1.0049 | 1.0067 |
| **9** | 0.9802 | 0.9835 | 0.9880 | 0.9893 | 0.9778 | 0.9777 | 0.9755 | 0.9732 | 0.9712 | 0.9734 |
| **10** | 0.9591 | 0.9628 | 0.9680 | 0.9694 | 0.9561 | 0.9562 | 0.9537 | 0.9511 | 0.9488 | 0.9514 |
| **11** | 1.0221 | 1.0253 | 1.0297 | 1.0309 | 1.0198 | 1.0195 | 1.0174 | 1.0153 | 1.0134 | 1.0155 |
| **12** | 0.9796 | 0.9829 | 0.9873 | 0.9886 | 0.9775 | 0.9769 | 0.9747 | 0.9725 | 0.9705 | 0.9727 |
| **13** | 1.0178 | 1.0210 | 1.0252 | 1.0265 | 1.0157 | 1.0152 | 1.0131 | 1.0109 | 1.0090 | 1.0111 |
| **14** | 0.9496 | 0.9538 | 0.9583 | 0.9598 | 0.9472 | 0.9466 | 0.9442 | 0.9417 | 0.9394 | 0.9419 |
| **15** | 0.9426 | 0.9465 | 0.9515 | 0.9528 | 0.9399 | 0.9395 | 0.9370 | 0.9345 | 0.9322 | 0.9347 |
| **16** | 0.9656 | 0.9692 | 0.9740 | 0.9754 | 0.9630 | 0.9628 | 0.9604 | 0.9580 | 0.9558 | 0.9582 |
| **17** | 0.9542 | 0.9580 | 0.9632 | 0.9646 | 0.9513 | 0.9514 | 0.9488 | 0.9462 | 0.9438 | 0.9464 |
| **18** | 0.9312 | 0.9353 | 0.9407 | 0.9422 | 0.9286 | 0.9280 | 0.9254 | 0.9226 | 0.9202 | 0.9229 |
| **19** | 0.9332 | 0.9373 | 0.9427 | 0.9442 | 0.9304 | 0.9301 | 0.9274 | 0.9246 | 0.9221 | 0.9249 |
| **20** | 0.9383 | 0.9423 | 0.9477 | 0.9492 | 0.9355 | 0.9352 | 0.9326 | 0.9298 | 0.9273 | 0.9301 |
| **21** | 0.9314 | 0.9354 | 0.9409 | 0.9423 | 0.9280 | 0.9281 | 0.9254 | 0.9227 | 0.9202 | 0.9229 |
| **22** | 0.9280 | 0.9321 | 0.9376 | 0.9389 | 0.9246 | 0.9247 | 0.9220 | 0.9193 | 0.9169 | 0.9196 |
| **23** | 0.9024 | 0.9066 | 0.9123 | 0.9133 | 0.8989 | 0.8986 | 0.8960 | 0.8933 | 0.8909 | 0.8936 |
| **24** | 0.8582 | 0.8628 | 0.8691 | 0.8697 | 0.8536 | 0.8535 | 0.8508 | 0.8481 | 0.8456 | 0.8483 |
| **25** | 0.7074 | 0.7127 | 0.7204 | 0.7192 | 0.7004 | 0.7003 | 0.6978 | 0.6953 | 0.6930 | 0.6955 |
| **26** | 0.6387 | 0.6441 | 0.6524 | 0.6509 | 0.6306 | 0.6305 | 0.6280 | 0.6255 | 0.6231 | 0.6257 |
| **27** | 0.6542 | 0.6597 | 0.6679 | 0.6660 | 0.6465 | 0.6465 | 0.6440 | 0.6416 | 0.6393 | 0.6418 |
| **28** | 1.0035 | 1.0060 | 1.0093 | 1.0105 | 1.0021 | 1.0021 | 1.0004 | 0.9985 | 0.9970 | 0.9988 |
| **29** | 0.6005 | 0.6014 | 0.6169 | 0.6131 | 0.5907 | 0.5906 | 0.5883 | 0.5860 | 0.5839 | 0.5862 |
| **30** | 0.5574 | 0.5613 | 0.5670 | 0.5666 | 0.5532 | 0.5532 | 0.5512 | 0.5492 | 0.5473 | 0.5493 |

## 6. Conclusion

Distribution sector reforms have made a significant impact on the operation and management of utility systems. DG sources play a key role in meeting the load demand, reducing power losses, and improving network management overall. In this study, the applications of the PSO and HPSO algorithms were presented to find the best location of DGs within a power network, with the objective of improving the voltage stability index and reducing power losses. Results showed that the proposed approach is a suitable and promising technique in solving the problem, but the best solutions found by PSO and HPSO and computational time can be improved by tuning the parameters and improving the mathematical model of the problem. Between these algorithms, HPSO is faster and its solutions are better in comparison with PSO. Because of the flexibility of these algorithms, further modeling requirements can be included in the fitness function to further improve the optimization design. For example, some of the initial simplifications can be removed from the design,

**Table 15.** Bus loadings in 5 time runs for the IEEE 30-bus system.

| Bus No. | $V_{after-install-DG}$ | | | | | | | | | |
|---|---|---|---|---|---|---|---|---|---|---|
| | PSO runs | | | | | HPSO runs | | | | |
| | *# 1* | *# 2* | *# 3* | *# 4* | *# 5* | *# 1* | *# 2* | *# 3* | *# 4* | *# 5* |
| **1** | 0 | 0 | 0 | 0 | 0 | 0 | 0 | 0 | 0 | 0 |
| **2** | 23.07 | 22.87 | 22.58 | 22.41 | 23.22 | 23.22 | 23.38 | 23.53 | 23.70 | 23.54 |
| **3** | 6.21 | 0.06.16 | 6.08 | 6.03 | 6.25 | 6.25 | 6.30 | 6.34 | 6.38 | 6.34 |
| **4** | 5.45 | 5.40 | 5.34 | 5.30 | 5.49 | 5.49 | 5.52 | 5.56 | 5.60 | 5.56 |
| **5** | 114.25 | 113.25 | 111.84 | 110.98 | 115.00 | 115.01 | 115.83 | 116.57 | 117.39 | 116.58 |
| **6** | 0 | 0 | 0 | 0 | 0 | 0 | 0 | 0 | 0 | 0 |
| **7** | 34.46 | 34.16 | 33.72 | 33.46 | 34.69 | 34.70 | 34.95 | 35.17 | 35.43 | 35.18 |
| **8** | 22.23 | 22.04 | 21.78 | 21.61 | 22.37 | 22.38 | 22.53 | 22.67 | 22.83 | 22.67 |
| **9** | 0 | 0 | 0 | 0 | 0 | 0 | 0 | 0 | 0 | 0 |
| **10** | 11.68 | 11.57 | 11.43 | 11.34 | 11.75 | 11.75 | 11.84 | 11.91 | 12.00 | 11.91 |
| **11** | 0 | 0 | 0 | 0 | 0 | 0 | 0 | 0 | 0 | 0 |
| **12** | 9.92 | 9.84 | 9.71 | 9.64 | 9.99 | 9.99 | 10.06 | 10.12 | 10.19 | 10.12 |
| **13** | 0 | 0 | 0 | 0 | 0 | 0 | 0 | 0 | 0 | 0 |
| **14** | 11.68 | 11.57 | 11.43 | 11.34 | 11.75 | 11.75 | 11.84 | 11.91 | 12.00 | 11.91 |
| **15** | 6.59 | 6.54 | 6.46 | 6.41 | 6.64 | 6.64 | 6.68 | 6.73 | 6.77 | 6.73 |
| **16** | 0.64 | 0.63 | 0.62 | 0.62 | 0.64 | 0.64 | 0.65 | 0.65 | 0.66 | 0.65 |
| **17** | 10.41 | 10.32 | 10.19 | 10.11 | 10.48 | 10.48 | 10.55 | 10.62 | 10.69 | 10.62 |
| **18** | 8.04 | 7.97 | 7.87 | 7.81 | 8.09 | 8.09 | 8.15 | 8.20 | 8.26 | 8.20 |
| **19** | 6.44 | 6.38 | 6.30 | 6.26 | 6.48 | 6.48 | 6.53 | 6.57 | 6.61 | 6.57 |
| **20** | 3.34 | 3.32 | 3.27 | 3.25 | 3.37 | 3.37 | 3.39 | 3.41 | 3.44 | 3.41 |
| **21** | 19.44 | 19.27 | 19.03 | 18.89 | 19.57 | 19.57 | 19.71 | 19.84 | 19.98 | 19.84 |
| **22** | 0 | 0 | 0 | 0 | 0 | 0 | 0 | 0 | 0 | 0 |
| **23** | 2.82 | 2.79 | 2.76 | 2.74 | 2.84 | 2.84 | 2.86 | 2.88 | 2.90 | 2.88 |
| **24** | 6.71 | 6.65 | 6.57 | 6.52 | 6.75 | 6.76 | 6.80 | 6.84 | 6.89 | 6.85 |
| **25** | 0 | 0 | 0 | 0 | 0 | 0 | 0 | 0 | 0 | 0 |
| **26** | 5.67 | 5.62 | 5.55 | 5.51 | 5.70 | 5.71 | 5.75 | 5.78 | 5.82 | 5.78 |
| **27** | 0 | 0 | 0 | 0 | 0 | 0 | 0 | 0 | 0 | 0 |
| **28** | 0 | 0 | 0 | 0 | 0 | 0 | 0 | 0 | 0 | 0 |
| **29** | 2.84 | 2.81 | 2.78 | 2.76 | 2.86 | 2.86 | 2.88 | 2.90 | 2.92 | 2.90 |
| **30** | 20.82 | 20.64 | 20.38 | 20.23 | 20.96 | 20.96 | 21.11 | 21.25 | 21.40 | 21.25 |

transforming the problem into a more realistic one. Future work will focus on increasing the number of devices to be installed, which implies finding a more suitable encoding method for the population.

# References


[1] R.B. Prada, L.J. Souza, "Voltage stability and thermal limit: constraints on the maximum loading of electrical energy distribution feeders", IEEE Proceedings Generation, Transmission and Distribution, Vol. 145, pp. 573-577, 1998.

[2] D. Liu, X. Xie, G. Mu, P. Li, "An on-line voltage stability index of power system based on synchronized phasor measurement", Proceedings of the CSEE, Vol. 25, pp. 13-17, 2005.

[3] P. Chiradeja, R. Ramakumar, "An approach to quantify the technical benefits of distributed generation", IEEE Transactions on Energy Conversion, Vol. 19, pp. 764-773, 2004.

[4] G.K. Morison, B. Gao, P. Kundur, "Voltage stability analysis using static and dynamic approaches", IEEE Transactions on Power Systems, Vol. 8, pp. 1159-1171, 1993.

[5] İ. Genç, Ö. Usta, "Impacts of distributed generators on the oscillatory stability of interconnected power systems", Turkish Journal of Electrical Engineering & Computer Sciences, Vol. 13, pp. 149-161, 2005.

[6] V. Miranda, "Wind power, distributed generation: new challenges, new solutions", Turkish Journal of Electrical Engineering & Computer Sciences, Vol. 14, pp. 455-473, 2006.

[7] T. Griffin, K. Tomsovic, D. Secrest, A. Law, "Placement of dispersed generation systems for reduced losses", Proceedings of the 33rd Annual Hawaii International Conference on System Sciences, pp. 1446-1454, 2000.

[8] N.S. Rau, Y.H. Wan, "Optimum location of resources in distributed planning", IEEE Transactions on Power Systems, Vol. 9, pp. 2014-2020, 1994.

[9] J.O. Kim, S.W. Nam, S.K. Park, C. Singh, "Dispersed generation planning using improved Hereford ranch algorithm", Electric Power Systems Research, Vol. 47, pp. 678-683, 1998.

[10] C. Wang, M.H. Nehrir, "Analytical approaches for optimal placement of distributed generation sources in power systems", IEEE Transactions on Power Systems, Vol. 19, pp. 2068-2076, 2004.

[11] P. Chiradeja, "Benefit of distributed generation: a line loss reduction analysis", IEEE/PES Transmission and Distribution Conference and Exhibition: Asia and Pacific, pp. 1-5, 2005.

[12] R.K. Singh, S.K. Goswami, "Optimum allocation of distributed generations based on nodal pricing for profit, loss reduction, and voltage improvement including voltage rise issue", International Journal of Electrical Power & Energy Systems, Vol. 32, pp. 637-644, 2010.

[13] P. Fríasa, T. Gómez, R. Cossent, J. Rivier, "Improvements in current European network regulation to facilitate the integration of distributed generation", International Journal of Electrical Power & Energy Systems, Vol. 31, pp. 445-451, 2009.

[14] T. Niknam, A.M. Ranjbar, A.R. Sirani, B. Mozafari, A. Ostadi, "Optimal operation of distribution system with regard to distributed generation: a comparison of evolutionary methods", IEEE Industry Applications Society Conference, Vol. 22, pp. 2690-2696, 2005.

[15] N. Mithulananthan, O. Than, P.L. Van., "Distributed generator placement in power distribution system using genetic algorithm to reduce losses", Thammasat International Journal of Science and Technology, Vol. 9, pp. 55-62, 2004.

[16] A. Keane, M. O'Malley, "Optimal allocation of embedded generation on distribution networks", IEEE Transactions on Power Systems, Vol. 20, pp. 1640-1646, 2005.

[17] K. Kyu-Ho, L.Y. Jeong, R.S Bong, L.S. Kuen, Y.S. Ku, "Dispersed generator placement using fuzzy-GA in distribution system", IEEE Xplore - Power Engineering Society Summer Meeting, pp. 1148-1153, 2002.

[18] G. Celli, E. Ghiani, S. Mocci, F. Pilo, "A multi-objective evolutionary algorithm for the sizing and sitting of distributed generation", IEEE Transactions on Power Systems, Vol. 20, pp. 750-757, 2005.

[19] K. Nara, Y. Hayashi, K. Ikeda, T. Ashizawa, "Application of tabu search to optimal placement of distributed generators", IEEE PES Winter Meeting, pp. 918-23, 2001.

[20] S.A. Taher, R. Hematti, A. Abdolalipour, S.H. Tabei, "Optimal decentralized load frequency control using HPSO algorithms in deregulated power systems", American Journal of Applied Sciences, Vol. 5, pp. 1167-1174, 2008.

[21] N. Shigenori, G. Takamu, Y. Toshiku, F. Yoshikazu, "A hybrid particle swarm optimization for distribution state estimation", IEEE Transactions on Power Systems, Vol. 18, pp. 60-68, 2003.

[22] P.Y Yint, S.S. Yu, P.P. Wang, Y.T. Wang, "A hybrid particle swarm optimization algorithm for optimal task assignment in distributed systems", Computer Standards & Interfaces Journal, Vol. 28, pp. 441-450, 2006.

[23] S.M. Kannan, P. Renuga, A. Rathina Grace Monica, "Optimal capacitor placement and sizing using combined fuzzy-HPSO method" , International Journal of Engineering, Science and Technology, Vol. 2, pp. 75-84, 2010.

[24] P.Y. Yin, S.S. Yu, P.P. Wang, Y.T. Wang, "Multi-objective task allocation in distributed computing systems by hybrid particle swarm optimization", Applied Mathematics and Computation, Vol. 184, pp. 407-420, 2007.

[25] A.E. Moneim Moussa, M.A.E. Gammal, A.Y. Abou-Ghazala, A.I. Attia, "A novel approach for unit commitment problem via an effective modified particle swarm optimization technique", European Journal of Scientific Research, Vol. 48, pp. 546-558, 2011.

[26] M.R. Aghamohamadi, M. Mohammadian, H. Saitoh, "Sensitivity characteristic of neural network as a tool for analyzing and improving voltage stability", IEEE/PES Transmission and Distribution Conference and Exhibition: Asia and Pacific, Vol. 2, pp. 1128-1132, 2002.

[27] M. Mohammadian, Power System Voltage Stability and Security Assessment by Neural Network Technique, MSc Thesis, K.N. Toosi University of Technology, 1997.

[28] M.R. Aghamohammadi, M. Mohammadian, "Loadability limit assessment in Iran power network with respect to voltage stability constrain," The 11th International Power System Conference, pp. 1-12, 1996.

[29] M.R. Aghamohammadi, M. Mohammadian, A. Golkar, "Generation scheduling constrained to voltage stability limit", The 16th International Power System Conference, 2001.

[30] M. Mohammadian, M.R. Aghamohammadi, S.M.T. Bathaee, "Power plants generation scheduling constrained to voltage stability limit based on sensivity characteristic of neural network", The 17th International Power System Conference, 2002.

[31] K.J. Binkley, New Methods of Increasing the Effectiveness of Particle Swarm Optimization, PhD Dissertation, Keio University, 2008.

[32] R.A. Hooshmand, M. Ezatabadipour, "Corrective action planning considering FACTS allocation and optimal load shedding using bacterial foraging oriented by particle swarm optimization algorithm", Turkish Journal of Electrical Engineering & Computer Sciences, Vol. 18, pp. 597-612, 2010.

[33] A.Z. Sevkli, F.E. Sevilgen, "StPSO: Strengthened particle swarm optimization", Turkish Journal of Electrical Engineering & Computer Sciences, Vol. 18, pp. 1095-1114, 2010.

[34] M. Tarafdar Hagh, S. Galvani, "Minimization of load shedding by sequential use of linear programming and particle swarm optimization", Turkish Journal of Electrical Engineering & Computer Sciences, Vol. 19, pp. 551-563, 2011.

[35] J. Kennedy, R.C. Eberhart, “Particle swarm optimization”, Proceedings of the IEEE International Conference on Neural Networks, pp. 1942-1948, 1995.

[36] T. Li, L. Xu, X.W. Shi, “A hybrid of genetic algorithm and particle swarm optimization for antenna design”, PIERS Online, Vol. 4, pp. 56-60, 2008.

[37] T.O. Ting, K.P. Wong, C.Y. Chung, “Hybrid constrained genetic algorithm/particle swarm optimization load flow algorithm”, IET Proceedings of Generation, Transmission & Distribution, Vol. 2, pp. 800-812, 2008.

[38] S. Jeong, S. Hasegawa, K. Shimoyama, S. Obayashi, “Development and investigation of efficient GA/PSO-hybrid algorithm applicable to real-world design optimization”, IEEE Computational Intelligence Magazine, pp. 36-44, 2009.

[39] F. Valdez, P. Melin, O. Castillo, “Evolutionary method combining particle swarm optimization and genetic algorithms using fuzzy logic for decision making”, Proceedings of the IEEE International Conference on Fuzzy Systems, pp. 2114-2119, 2009.

[40] R. Bhuvaneswari, V.P. Sakthivel, S. Subramanian, G.T. Bellarmine, “Hybrid approach using GA and PSO for alternator design”, Proceedings of the IEEE International Southeastcon, pp. 169-174, 2009.

[41] R.F. Abdel-Kader, “Genetically improved PSO algorithm for efficient data clustering”, Proceedings of International Conference on Machine Learning and Computing, pp. 71-75, 2010.